Le 2ème Séminaire International sur les Energies Nouvelles et Renouvelables
The 2nd International Seminar on New and Renewable Energies
Unité de Recherche Appliquée en Energies Renouvelables,
Ghardaïa – Algérie 15, 16 et 17 Octobre 2012

# Optimisation of A Photovoltaic Pumping System Destined to Supply Drinking Water

K. Amokrane
*Laboratory L.T.I.I*
*Department of Electrical Engineering University of Bejaia (Algeria)*
Ka_amok76@yahoo.fr

*Abstract:* PV energy is used in different applications and especially in water pumping and irrigation in remote areas. However, the performances of a photovoltaic pumping system can be degraded with variations of solar radiation. In order to maximize the efficiency of the photovoltaic energy system, it is necessary to track the maximum power point of the PV array. Many methods have been developed to determine the maximum power point (MPP). In this paper we present the results of performance optimization of a PV pumping system anther Bejaia (Algeria) climate condition. The pumped water is used to satisfy the domestic needs of three different families during three consecutive years (2008 to 2010). The proposed system is illustrated. It consists of PV arrays, a motor-pump with two configurations of AC and DC pumps and a maximum power point tracker. Batteries are added for the purpose of ensuring continuous power flow. The storage battery model used is presented with obtained measurement results. Simulation is developed under Matlab-Simulink Package. Some experimental results are also given to show the effectiveness of the studied system.
*Keywords:* Photovoltaic systems, Pumping, Maximum power point tracker, simulation, Storage battery.

## I. INTRODUCTION

Solar energy which is free and abundant in most parts of the world has proven to be an economical source of energy in many applications. Algeria receives large quantities of solar radiations all over the year and PV pumping is clearly the solution to the water problem in remote sites. Currently, in Algeria, the number of photovoltaic energy-driven water pumps is very low. The main obstacles to the PV pumping development and dissemination are the high initial investment, the low awareness about these systems and the lack of tools serving to predict their performances. The climate varies from the Mediterranean type in the north to the desert type in the south. Algeria with a total area of 2,381,741 km$^2$, can be divided into three climatic regions which run parallel to each other horizontally through the country [01].

In this paper, we present performance optimization results of a PV pumping system in Bejaia (Algeria) climate. The pumped water is desired to satisfy the domestic needs of three different families during three consecutive years (2008-2010). The proposed system consists of PV arrays, a motor-pump with two possible configurations of AC and DC pumps, a storage tank and a controller to track maximum power. The paper is organized as follows. In Section II, we present the photovoltaic pumping system with the two configurations and the battery storage used. Mathematical relations between the essential variables of a PV system are presented. These relations are necessary for simulating its operation under different irradiance and temperature levels. Three different models are presented [02] and simulations results are compared to experimental measures. The control system is required to track maximum power whatever environmental conditions variations. An MPPT method is developed in order to track the MPP of a PV system. The modeling of the subsystem pumping is given with the two cases of AC and DC motor. The storage battery model used is presented with obtained measurement results.

Section III is devoted to Solar potential and the water needs in Bejaia (Algeria). The pumped water is desired to satisfy the domestic needs of three different families during three consecutive years (2008-2010).

Finally the experimental bench is presented in section IV and some experimental results are presented and compared to simulation ones achieved using the MATLAB®-SIMULINK® package.

## II. SYSTEM DESCRIPTION

### A. *Description*

A general photovoltaic pumping system consists of PV arrays, a boost chopper working as a maximum power point tracker (MPPT), an inverter and a motor driving a centrifugal pump. In fig.1, we present a scheme with two possible configurations of AC and DC pumps.

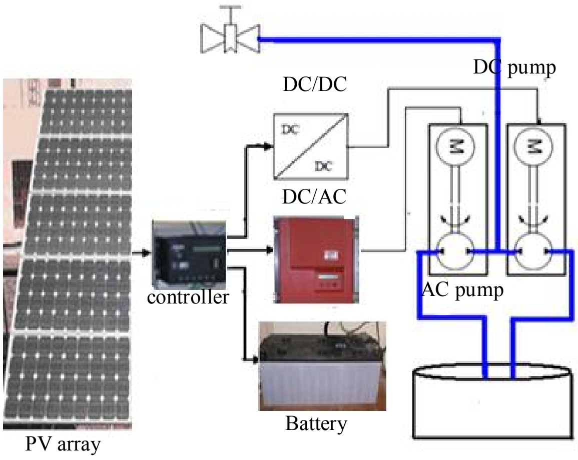


Fig.1 Description of the PV pump system

### A. *Modeling of photovoltaic generator*

In literature, there are several mathematical models that describe the operation and behavior of the photovoltaic generator [4]. These models differ in the calculation procedure, accuracy and the number of parameters involved in the calculation of the current-voltage characteristic.

### *B.1 First model:*

The model is called one diode and the equivalent circuit (Fig 2) consists of a single diode for the cell polarization phenomena and two resistors (series and shunt) for the losses.

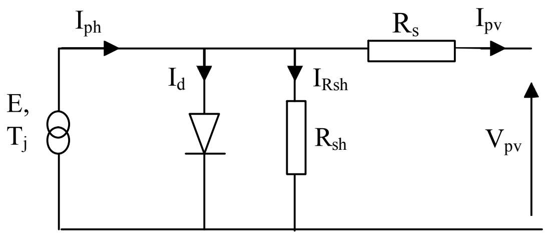


Fig 2.Simplified equivalent circuit of solar cell

$I_{pv}(V_{pv})$ characteristic of this model is given by the following equation [5]:

$$I_{pv} = I_{ph} - I_d - I_{Rsh} \tag{1}$$

$$I_{pv} = I_{ph} - I_0\left[e^{q\frac{(V_{pv}+I_{pv}.R_s)}{AkT_j}} - 1\right] - \frac{V_{pv}}{R_{sh}} \tag{2}$$

The photocurrent, $I_{ph}$, is directly dependent upon both insolation and panel temperature, and may be written in the following form:

$$I_{ph} = P_1.E.\left[1 + P_2.(E - E_{ref}) + P_3.(T_j - T_{ref})\right] \tag{3}$$

Where*:* $E$ insolation in the panel plane (W/m²); $E_{ref}$ corresponds to the reference insolation of 1000 W/m² and $T_{jref}$ to the reference panel temperature of 25°C. $P_1$, $P_2$ and $P_3$ are constant parameters.

The polarization current $I_d$ of junction PN, is given by the expression:

$$I_d = I_0.[\exp(\frac{q.(V_{pv} + R_s.I_{pv})}{A.n_s.k.T_j}) - 1] \tag{4}$$

With: $I_0$ (A) saturation current, q the elementary charge (ev), k Botzman's constant, A ideality factor of the junction, $T_j$ : junction temperature of the panels (°K) and $R_s$, $R_{sh}$ (Ω) resistors (series and shunt).

### *B.2 Second Model*

The PV array equivalent circuit current $I_{pv}$ can be expressed as a function of the PV array voltage $V_{pv}$:

$$I_{pv} = I_{sc}\left\{1 - C_1\left[\exp C_2 V_{pv}^m - 1\right]\right\} \tag{5}$$

Where the coefficients $C_1$, $C_2$ and m are defined as:

$$C_1 = 0.01175 \tag{6}$$

$$C_2 = \frac{C_4}{V_{oc}^m} \tag{7}$$

$$C_3 = \ln\left[\frac{I_{sc}(1 + C_1) - I_{mpp}}{C_1 I_{sc}}\right] \tag{8}$$

$$C_4 = \ln\left[\frac{1 + C_1}{C_1}\right] \tag{9}$$

$$m = \frac{\ln\left[\frac{C_3}{C_4}\right]}{\ln\left[\frac{V_{mpp}}{V_{oc}}\right]} \tag{10}$$

With: $V_{mpp}$ voltage at maximum power point; $V_{oc}$ open circuit voltage; $I_{mpp}$ current at maximum power point; $I_{sc}$ short circuit current.

Equation (5) is only applicable at one particular insolation level E, and cell temperature, $T_j$, at standard test conditions (STC) (E=1000 W/m², $T_j$=25 °C). When insolation and temperature vary, the parameters change according to the following equations:

$$\Delta T_j = T_j - T_{jref} \tag{11}$$

$$\Delta I_{pv} = \alpha_{sc}\left(\frac{E}{E_{ref}}\right)\Delta T_j + \left(\frac{E}{E_{ref}} - 1\right) I_{sc,ref}$$

(12)

$$\Delta V_{pv} = -\beta_{oc}\Delta T_j - R_s \Delta I_{pv} \tag{13}$$

Where: $\alpha_{sc}$ current temperature coefficient; $\beta oc$ voltage temperature coefficient

The new values of the photovoltaic voltage and the current are given by:

$$V_{pv,new} = V_{pv} + \Delta V_{pv} \quad (14)$$

$$I_{pv,new} = I_{pv} + \Delta I_{pv} \quad (15)$$

*B.3 Third model*

In the model "two diodes", the two diodes are present for the PN junction polarization phenomena. These diodes represent the recombination of the minority carriers, which are located both at the surface of the material and within the volume of the material (Fig.3.).

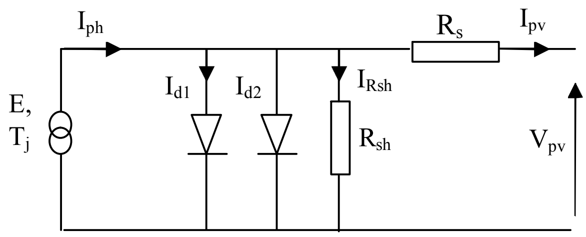


Fig.3 Equivalent circuit for two diode model

The following equation is then obtained:

$$I_{pv} = I_{ph} - (I_{d2} + I_{d2}) - I_{Rsh} \quad (16)$$

with $I_{ph}$ and $I_{Rsh}$ maintaining the same expressions as above (Eq.2). For the recombination currents, we have:

$$I_{d1} = I_{01}\left[\exp\left(\frac{q.(V_{pv}+R_S.I_{pv})}{A.n_s.k.T_j}\right)-1\right] \quad (17)$$

$$I_{d2} = I_{02}\left[\exp\left(\frac{q.(V_{pv}+R_S.I_{pv})}{2.A.n_s.k.T_j}\right)-1\right] \quad (18)$$

The saturation currents are written as:

$$I_{01} = P_4.T_j^3.\exp\left(\frac{-E_g}{k.T_j}\right) \quad (19)$$

$$I_{02} = P_5.T_j^3.\exp\left(\frac{-E_g}{2.k.T_j}\right) \quad (20)$$

With $n_s$ is the number of cells in branched series, $E_g$ represents the gap energy

The final equation of the model is thereby written as:

$$I_{pv} = P_1.E.[1 + P_2.(E - E_{ref}) + P_3.(T_j - T_{ref})] - \frac{(V_{pv} + R_s.I_{pv})}{R_{sh}}$$
$$- P_{04}.T_j^3.\exp\left(\frac{-E_g}{k.T_j}\right)\left[\exp\left(q.\frac{V_{pv}+R_s.I_{pv}}{A.n_s.k.T_j}\right)-1\right] \quad (21)$$
$$- P_{14}.T_j^3.\exp\left(\frac{-E_g}{2.k.T_j}\right)\left[\exp\left(q.\frac{V_{pv}+R_s.I_{pv}}{2.A.n_s.k.T_j}\right)-1\right]$$

Figure 4 show the current/voltage characteristics obtained using the three models compared with the experimental values corresponding to a 110 Wc Siemens panel (Table 1.)

TABLE.1
Parameter of the PV panel SIEMENS SM110-24[ ]

| | |
|---|---|
| $P_{PV}$ | 110W |
| $I_{mpp}$ | 3.15A |
| $V_{mpp}$ | 35V |
| $I_{sc}$ | 3.45A |
| $V_{oc}$ | 43.5V |
| $\alpha_{sc}$ | 1.4mA/°C |
| $\beta_{oc}$ | -152mV/°C |
| $P_{mpp}$ | 110W |

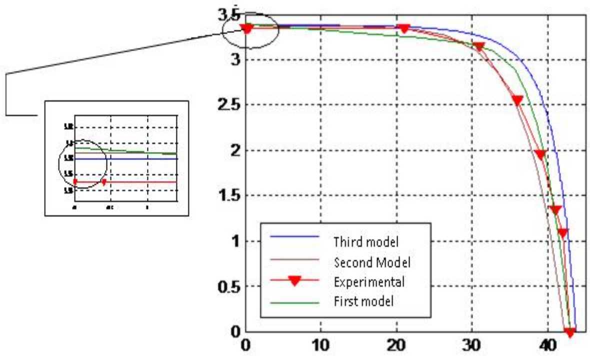


Fig 4. $I_{pv}(V_{pv})$ characteristics of 110 Wc Pannel.

*B. Modeling subsystem pumping*

*C.1 Pump model*

Many different varieties of pumps are used with PV-pumping system. In our case, we use the model expresses the water flow output (Q) directly as a function of the electrical power input (P) to the motor-pump, for different total heads. A polynomial fit of the third order expresses the relationship between the flow rate and power input, as described by the following equation [6, 7]:

$$P(Q,h) = a(h)Q^3 + b(h)Q^2 + c(h)Q + d(h) \quad (22)$$

Where P is the electrical power input of the motor-pump, h is the total head and a(h), b(h), c(h), d(h) are the coefficients corresponding to the working total head.

$$a(h) = a_0 + a_1h^1 + a_2h^2 + a_3h^3 \quad (23)$$

$$b(h) = b_0 + b_1h^1 + b_2h^2 + b_3h^3 \quad (24)$$

$$c(h) = c_0 + c_1h^1 + c_2h^2 + c_3h^3 \quad (25)$$

$$d(h) = d_0 + d_1h^1 + d_2h^2 + d_3h^3 \quad (26)$$

With: $a_i$, $b_i$, and $d_i$ constants which depend on the type of sub-solar pumping system.

The calculation of the instantaneous flow in terms of power is calculated using Newton-Raphson method.

Thus at the k$^{th}$ iteration, the flow Q is given by the following equation:
For d – Pa (Q)> 0:

$$Q_k = Q_{k-1} - \frac{F(Q_{k-1})}{F'(Q_{k-1})} \quad (27)$$

With:

$$F(Q_{k-1}) = aQ^3_{k-1} + bQ^2_{k-1} + cQ_{k-1} + d - P_a(Q_{k-1}) \quad (28)$$

Where:
$F'(Q_{k-1})$ is the derivative of the function $F(Q_{k-1})$

*C.2 A.C motor*

We use an induction motor which is modeled using voltage and flux equations referred in a general frame:

-Stator voltage equations:

$$\begin{cases} V_{Sd} = R_S I_{Sd} + \dfrac{d\Phi_{Sd}}{dt} \\ V_{Sq} = R_S I_{Sq} + \dfrac{d\Phi_{Sq}}{dt} \end{cases} \quad (29)$$

Where: $(I_{sd}\ I_{sq})$, $(V_{sd},\ V_{sq})$ and $(\Phi_{sd},\ \Phi_{sq})$ are the (d,q) components of the stator current, voltage and flux, $R_s$ is the stator resistance.
-Rotor voltage equations:

$$\begin{cases} 0 = V_{Rd} = R_R I_{Rd} + \dfrac{d\Phi_{Rd}}{dt} + \dfrac{d\theta}{dt}\Phi_{Rq} \\ 0 = V_{Rq} = R_R I_{Rq} + \dfrac{d\Phi_{Rq}}{dt} - \dfrac{d\theta}{dt}\Phi_{Rd} \end{cases} \quad (30)$$

Where: $I_{Rd}$, $I_{Rq}$ are (d,q) rotor current, $\Phi_{Rd}$, $\Phi_{Rq}$ are (d,q) rotor flux, $R_r$ is the rotor resistance.

We obtain the follow mathematical model:

$$\begin{bmatrix} \frac{di_{ds}}{dt} \\ \frac{di_{qs}}{dt} \\ \frac{di_{dr}}{dt} \\ \frac{di_{qr}}{dt} \end{bmatrix} = \frac{1}{\sigma}\begin{bmatrix} -\frac{R_s}{L_s} & \frac{P\cdot\omega_r\cdot L_m^2}{L_s\cdot L_r} & \frac{L_m R_r}{L_s\cdot L_r} & \frac{P\cdot\omega_r\cdot L_m}{L_s} \\ -\frac{P\cdot\omega_r\cdot L_m^2}{L_s\cdot L_r} & -\frac{R_s}{L_s} & \frac{P\cdot\omega_r\cdot L_m}{L_s} & \frac{L_m R_r}{L_s\cdot L_r} \\ \frac{L_m R_s}{L_s\cdot L_r} & -\frac{P\cdot\omega_r\cdot L_m}{L_r} & -\frac{R_r}{L_r} & -P\omega_r \\ \frac{P\cdot\omega_r\cdot L_m}{L_r} & \frac{L_m R_s}{L_s\cdot L_r} & P\omega_r & -\frac{R_r}{L_r} \end{bmatrix}\begin{bmatrix} i_{ds} \\ i_{qs} \\ i_{dr} \\ i_{qr} \end{bmatrix}$$

$$+\frac{1}{\sigma}\begin{bmatrix} \frac{1}{L_s} & 0 \\ 0 & \frac{1}{L_s} \\ -\frac{L_m}{L_s L_r} & 0 \\ 0 & -\frac{L_m}{L_s L_r} \end{bmatrix}\begin{bmatrix} V_{ds} \\ V_{qs} \end{bmatrix} \quad (31)$$

With : $\sigma$ is the leakage coefficient

- Mechanical equation:

$$T_{motAC} - T_{Load} = J_{motAC}\cdot\frac{d\omega_{rAC}}{dt} \quad (32)$$

With: $\omega_{rAC}$ is the AC motor velocity angular, $J_{motAC}$ the inertia of the AC motor.

The electromagnetic torque can be written as:

$$T_{motAC} = P.(\phi_{sd}.i_{sq} - \phi_{sq}.i_{sd}) \quad (33)$$

Where: P is the pole pair number of the AC machine.

*C.3 DC Motor*

By neglecting the induced reaction and the switching phenomenon; the motor voltage will be equal to:

$$V_{motDC} = R_a.I_{mot} + L_a.\frac{dI_{mot}}{dt} + K_{mot}.\omega_{rDC} \quad (34)$$

The mechanical equations are:

$$T_{motDC} = K_{mot}.I_{mot} \quad (35)$$

The torque of the centrifugal pump is given as:

$$T_{load} = K_{load}.\omega_{rDC}^2 + T_S \quad (36)$$

Where: $T_{load}$ the load torque (N.m), $T_{motDC}$ the motor torque. (Nm), $K_e$ the emf constant (V/(rd.s$^{-1}$)), $K_{mot}$ the constant torque (Nm/A) and $K_{load}$ (Nm/rad.s-1)² is a load Torque coefficient.
And we have.

$$T_{motDC} - T_{Load} = J_{motDC}\cdot\frac{d\omega_{rDC}}{dt}$$

With: $\omega_{rDC}$ is the DC motor velocity angular, $J_{motDC}$ the inertia of the DC motor.

*C. Controller*

The MPPT is necessary to draw the maximum amount of power from the PV module. In our work, we use the Perturb and Observ (P&O) algorithm . In this strategy, the voltage is perturbed by a small increment and the resulting change in power is observed. If the change in power is positive, the voltage is adjusted by the same increment and the power is again observed. This continuous until the change in power is negative, at which point the direction of the change is reversed From the simulations results, it is clear that the operating point of this system operates closer to a maximum power point for variations in irradiation and temperature (Fig 12a and Fid 12b)

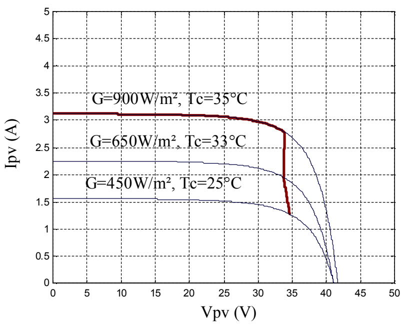


Fig.12a Power-voltage characteristic of a PV module for different irradiance.

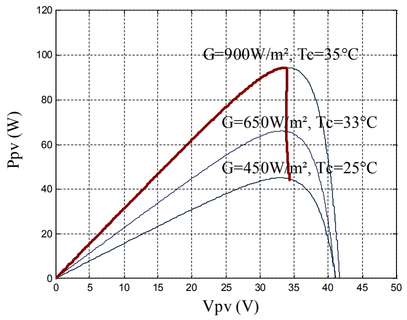


Fig.12b Current-voltage characteristic of a PV module for different irradiance.

## E. *Battery bank.*

We opted for the CIEMAT model. It is characterized by setting a series of women with a variable resistor (Fig.14). The characteristics of the source voltage $E_b$ and internal resistance $R_b$ depend on temperature and battery charge state.

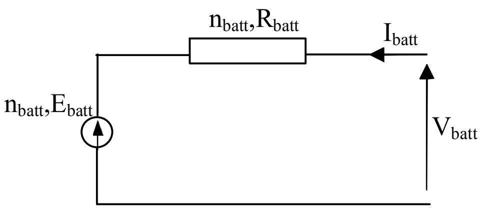


Fig.14. Equivalent circuit model CIEMAT

For a number $n_b$ of cell, voltage equation is:

$$V_{batt} = n_{batt}.E_{batt} \pm n_{batt}.R_{batt}.I_{batt} \qquad (35)$$

With :$V_{batt}$ : battery voltage, $I_{batt}$ : battery current., $E_{batt}$ : electromotive force depending on the battery charge state., $R_{batt}$ : internal resistance which varies with the state of charge.

The battery behaves as complex impedance $Z_{batt}$ containing a resistance $R_{batt}$ and a reactance $X_{batt}$ to this disturbance.

$$Z_{batt} = R_{batt} - jX_{batt} \qquad (36)$$

The module of the complex impedance is thus well defined by the ratio of the absolute values of the two signals. We deduce the dephasing by the temporal difference between the two signals with the passage by zero. Knowing the module of $Z_{batt}$ and dephasing, we can thus deduce the real part $R_{batt}$ and imaginary $X_{batt}$ of the impedance for his state of charge, these values changes according to the latter. We obtain:

| $R_{batt}$ | $X_{batt}$ | $C_{batt}$ |
|---|---|---|
| 0.577Ω | 0.15Ω | 21.22mF |

We give some simulation results (Fig17-20).

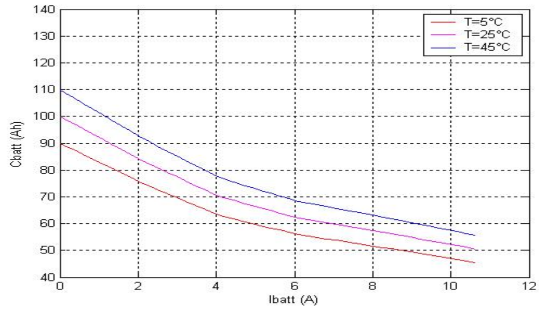


Fig17. Battery capacity variation for different temperatures.

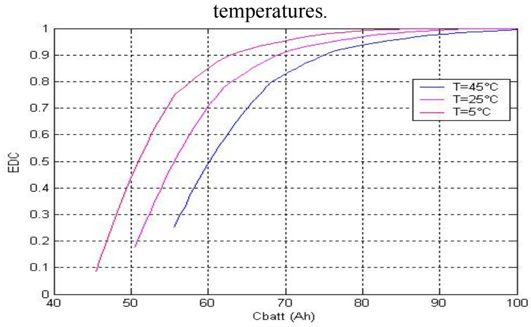


Fig 18. Variation of the state charge for different temperatures

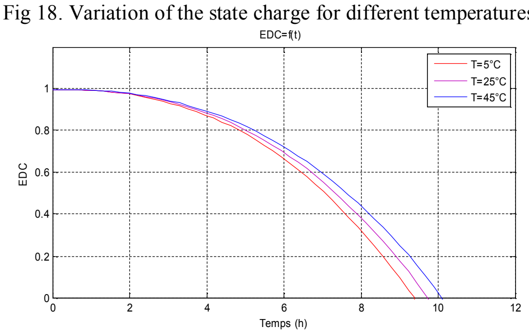


Fig 19. Variation of the charge state according to the discharge time for different temperatures

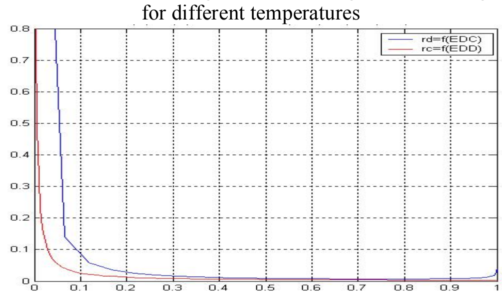


Fig 20. Variation of load and discharge voltage according to EDD and EDC

We note that when the temperature increases, the behavior of the battery is saved by increased as well. The value of the battery internal resistance decreases rapidly with increasing temperature, which is mainly due to the change of electrolyte resistance.

## III. SOLAR POTENTIAL IN BEJAIA (ALGERIA)

Due to its geographical location, Algeria has one of the highest solar fields in the world. Regarding the region of Bejaia (36°43' N 5°04' E 2 m), which is a coastal city (Fig.10) in the North East of Algeria.

The results were carried out using measured meteorological data for Bejaia We present the average daily sunshine for three seasons (winter, spring and summer) We note an average daily radiation exceeding 5kWh/m2/jour (Fig. 21).

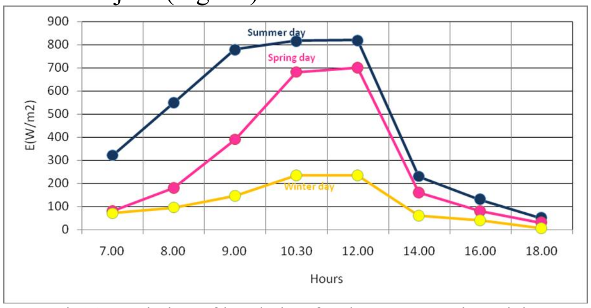


Fig21. Variation of insolation for three seasons in Bejaia

Conventional water, generated by rainfall, represents the most important potential. In Bejaia, precipitations, which mainly occur in winter and the beginning of spring, are very irregular with considerable variations from year to year. The average precipitations are 1600 mm/year.

## IV.SIMULATION OF PUMPING SYSTEM

### *A. Simulation of the two pumping System*

The performance of pumping systems are calculated using a PV generator 550Wc with a configuration of a branch of SIEMENS MS 5 modules in series 24V 110W (5S x 1p). The peak power of the photovoltaic module is 110 W. This generator feeds both subsystems pumping SP1 or SP2: The SP1 system consists of a DC motor and a pump progressive cavity. The SP2 system consists of a three phase AC motor and a multistage centrifugal pump. The results simulation performance for the two systems (for a selected height h = 7m) is presented in Fig.23 and Fig.24. We note on the figures 23 and 24 that the water volume of water pumped by the two systems is important during the summer and lowest during the winter. The latter is due to the variation of solar radiation is also higher in summer than in spring and winter.

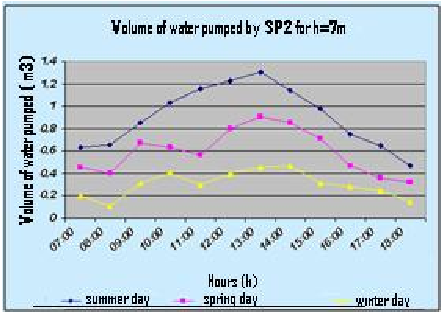


Fig.23. Volume of water pumped daily (spring, summer, winter) with SP2, h = 7m

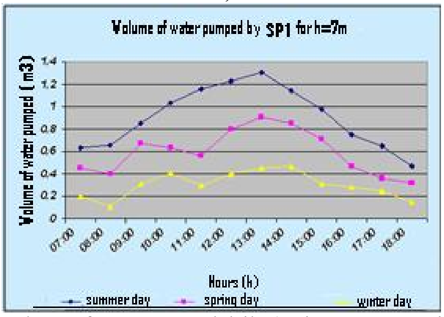


Fig.24. Volume of water pumped daily (spring, summer, winter) by SP1, h= 7m

The varying amount of water pumped by both SP1 and SP2 systems during 2010 is illustrated in Figure 25. We remark that the flow is greatest during the months (June, July, August) and minimum during the month of December. We also note that the quantity of water pumped by the SP1 is more important than that pumped by SP2.

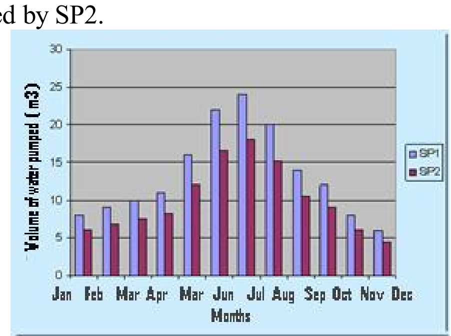


Fig.25. Volume of water pumped annually (2010), h = 7m

### *B. Application to domestic needs:*

The pumped water is desired to satisfy the domestic needs of three different families during three consecutive years (2008-2010)

Fristly, we consider la consummation of each family during the three seasons of the three considered years.

Table5.
Consummation of three families.

| Year | Season | Consummation (m3) | | |
|---|---|---|---|---|
| | | Family N°1 | Family N°2 | Family N°3 |
| | Winter | 23 | 20 | 14 |
| | Springer | 27 | 23 | 18 |
| 2008 | Summer | 51 | 28 | 24 |
| Total | | 101 | 71 | 56 |
| | Winter | 24 | 22 | 24 |
| | Springer | 28 | 25 | 28 |
| 2009 | Summer | 42 | 30 | 37 |
| Total | | 94 | 77 | 89 |
| | Winter | 24 | 20 | 15 |
| | Springer | 28 | 26 | 26 |
| 2010 | Summer | 45 | 29 | 39 |
| Total | | 97 | 75 | 80 |

## V. CONCLUSION

Generally, pumping systems consist of a photovoltaic generator and a sub-pump system. These systems operate over the sun without electrochemical storage. The water pumped can be used directly or stored in a tank for future use. This type of water storage is the most solution widely adopted over the storage in electrochemical batteries. The power conditioning system's main role is to optimize the transfer of power between the photovoltaic generator and the motor-pump group. The power conditioning system may be a converter dc/ac to an AC motor or a dc/dc converter for a DC motor.

In this work, we have simulated and tested the operation of pumping systems destined to supply drinking water. Analysis of results allowed us to compare the performance of two types of pumping systems for different technology. The performances are compared in terms of total height and geographical site of Bejaia (Algeria). We can conclude that the system SP1 give the best results.

The results show that the performance of the photovoltaic pumping system depends deeply on the pumping total head and the peak power of the photovoltaic array.

## REFERENCES

[1] A. Hamidat A. Hadj Arab and MT Boukadoum, Performance and costs of PV pumping systems in Algeria, Renewable Energy. Vol. 8 (2005) 157 - 166

[2] A. Hamidat, 'Outlook for Large PV Pumping and Low Depths', Proceedings of the National Days of Technical Studies and Explo itation on Solar Energy, ENA, Algiers, June 29 to 30, 1996.

[3] C. Franx, 'A New Approach to Using Solar PumpSystems Submersible Motors', Proceedings of the 2nd Photovoltaic Solar Energy Conference, pp. 1038 - 1045, 1979.

[4] D.S.H. Chan, J. R. Philips and J.C.H. Phang, 'A Comparative Study of Extraction Methods for Solar Cell Model Parameters' Solid State Electronics, Vol. 29, No. 3, pp. 329-337, 1986.

[5] L. Keating, D. Mayer, S. McCarthy and GT Wrixon, "Concerted Action on Computer Modelling and Simulation ', Proceedings of the 10th European Photovoltaic Solar Energy Conference, Lisbon, Portugal, pp. 1259 - 1265, 1991.

[6] A. Hamidat, 'Simulation of Photovoltaic Pumping Systems Intended for Food and Drinking Water and Irrigation for Small', PhD thesis, University Abou Bakr Belkaid, Tlemcen, 2004.

[7] A. Hamidat, 'Simulation of the Performance and Cost Calculations of the Surface Pump', Renewable Energy, Vol. 18, pp.383-392,1999.

.